Electrochemical and Solid-State Letters, **8** (1) J1-J3 (2005)
1099-0062/2004/8(1)/J1/3/$7.00 © The Electrochemical Society, Inc.

Nonlinear Electrical Properties of Grain Boundaries in Oxygen Ion Conductors: Acceptor-Doped Ceria

Xin Guo,[z] Shaobo Mi, and Rainer Waser

Institut für Festkörperforschung, Forschungszentrum Jülich, 52425 Jülich, Germany

Owing to the positively charged grain boundary cores in acceptor-doped ZrO_2 and CeO_2, oxygen vacancies are depleted in the space charge layers. The validity of this space charge concept was checked for Y_2O_3-doped CeO_2 ceramic of high purity. Electrical fields up to 2×10^5 V cm^{-1} were applied to the grain boundaries of 1.0 mol % Y_2O_3-doped CeO_2 at 400°C in air, and the grain boundary properties were separated by means of impedance spectroscopy. It was discovered that the current-voltage relation for individual grain boundary was nonlinear, and that the effective grain boundary thickness increased with increasing bias, which supports the space charge concept.
 [DOI: 10.1149/1.1830393]

Manuscript received April 23, 2004. Available electronically November 22, 2004.

Over a wide temperature and oxygen partial pressure range acceptor-doped ZrO_2 and CeO_2 are pure oxygen ion conductors, with oxygen vacancies being the charge carriers. The specific grain boundary conductivity of acceptor-doped ZrO_2 and CeO_2 is several orders of magnitude lower than the bulk conductivity.[1-6] This low grain boundary conductivity has usually been attributed to an intergranular siliceous phase.[1,2] However, the ionic conduction across the grain boundaries actually occurs solely through the direct grain-to-grain contacts;[5,6] the presence of the siliceous phase only determines the fraction of the grain-to-grain contacts and constricts the ionic current across the grain boundaries. However, in ZrO_2 and CeO_2 materials of high purity in which a siliceous phase was not observed, the specific grain boundary conductivity was measured to be still orders of magnitude lower than that of the bulk.[3-6] It is thus obvious that the grain-to-grain contacts, whose electrical properties are determined by the charge carrier distribution there, are themselves electrically resistive.

In the core-space charge layer model,[7] a grain boundary consists of a grain boundary core (crystallographic mismatch zone) and two adjacent space charge layers. In 2 mol % Y_2O_3-doped ZrO_2, the enrichment of additionally added divalent and trivalent minority solutes at the grain boundaries was found to be significant, whereas the enrichment of pentavalent minority solutes was not observed,[8] demonstrating a positive potential in the ZrO_2 grain boundary core. Gadolinium has almost perfect match of ionic radius in the CeO_2 lattice, therefore, the elastic strain resulting from the ion size mismatch is too small to be an effective segregation driving force; any Gd (*i.e.*, Gd'_{Ce}) segregation at the CeO_2 grain boundaries is mostly driven by the Coulomb interaction with a positive charge. The grain boundary segregation of Gd in Gd_2O_3-doped CeO_2 was observed,[9] being in accordance with the expected positive core potential. Molecular dynamics simulations of a $\Sigma 5$ symmetrical tilt grain boundary in Y_2O_3-doped ZrO_2 shows that the structure relaxation can produce intrinsic oxygen vacancies in the grain boundary core.[10] Electron energy-loss spectroscopy (EELS) investigations of the grain boundaries in Y_2O_3-doped ZrO_2 show a decrease in the O/Zr and O/Y ratios,[11] indicating an enhanced oxygen vacancy concentration in the grain boundary core. Studies of the grain boundaries in Gd_2O_3-doped CeO_2 ceramic samples reveal similar changes in the O/Ce ratio,[11] indicating that these effects may be generic to the grain boundaries in fluorite-structured materials. The high concentration of oxygen vacancies in the grain boundary cores of acceptor-doped ZrO_2 and CeO_2 may account for the positive core charge.

The positively charged grain boundary cores of acceptor-doped ZrO_2 and CeO_2 expel oxygen vacancies; the charge carriers are therefore depleted in the space charge layers. The space charge depletion successfully explains the electrical properties of the grain-to-grain contacts.[5,6,12,13] In particular, when subjecting ZrO_2 to external mechanical loads, the bulk and grain boundary electrical responses were found to be almost identical, indicating that the space charge layers are responsible for the grain boundary electrical responses.[14,15] Because a space charge layer is a part of the bulk from a crystallographic point of view, but electrically it is a part of the grain boundary.

At equilibrium and zero bias state the two space charge layers of a grain boundary are symmetrical; but after applying a dc bias voltage, one space charge layer is depressed, while the other one is extended. Such a situation should cause nonlinear grain boundary electrical properties under dc bias voltage. To conclusively prove the concept of space charge depletion, the nonlinear grain boundary electrical properties under dc bias voltage should be demonstrated. Tanaka *et al.*[16] attempted to demonstrate the nonlinear grain boundary electrical properties, but failed to detect the subtle voltage dependence of the space charge layers, probably because the thick intergranular siliceous phase in their samples strongly masked the effects of the space charge layers. It was previously discovered that the grain boundary resistance is dominant in 1.0 mol % Y_2O_3-doped CeO_2.[6] When applying a bias to such a sample, the bias could mostly drop over the grain boundaries. If the grain size of the sample is large enough, then the bias over a single grain boundary can be considerable, providing us a unique chance to investigate the nonlinear grain boundary properties. Such an investigation is reported in this paper.

Experimental

1.0 mol % Y_2O_3-doped CeO_2 ceramic samples, with 98% of the theoretical density and an average grain size of 35 μm, were prepared from CeO_2 powder and Y_2O_3 powder, both with 99.999% purity (Aldrich Chemical Co. Inc., Milwaukee, WI), by pressing and sintering at 1650°C in air for 15 h. The phase of the samples was confirmed by X-ray diffraction to be cubic. The microstructure was investigated by means of scanning electron microscopy (SEM, Hitachi model S-4100), and high-resolution transmission electron microscopy (HRTEM, Philips model CM20 ST, operating at 200 kV). The SEM investigations were carried out on polished and thermally etched surfaces, and average grain sizes (d_g) were determined. The HRTEM samples were prepared by standard methods, involving mechanical grinding to a thickness of about 0.1 mm, dimpling to ~10 μm, then ion-beam milling to electron transparency. The electrical properties were investigated by impedance spectroscopy, performed at 400°C in air at amplitude of 100 mV (1260 frequency-response analyzer, in conjunction with 1296 dielectric interface, Solartron Instruments, Farnborough, U.K.). The measured impedance spectra were fitted according to an equivalent circuit consisting of three *RQ* circuits in series. Here *R* represents a resistance, *Q* a constant phase element. Platinum paste was used to fabricate the porous electrodes.

[z] E-mail: x.guo@fz-juelich.de

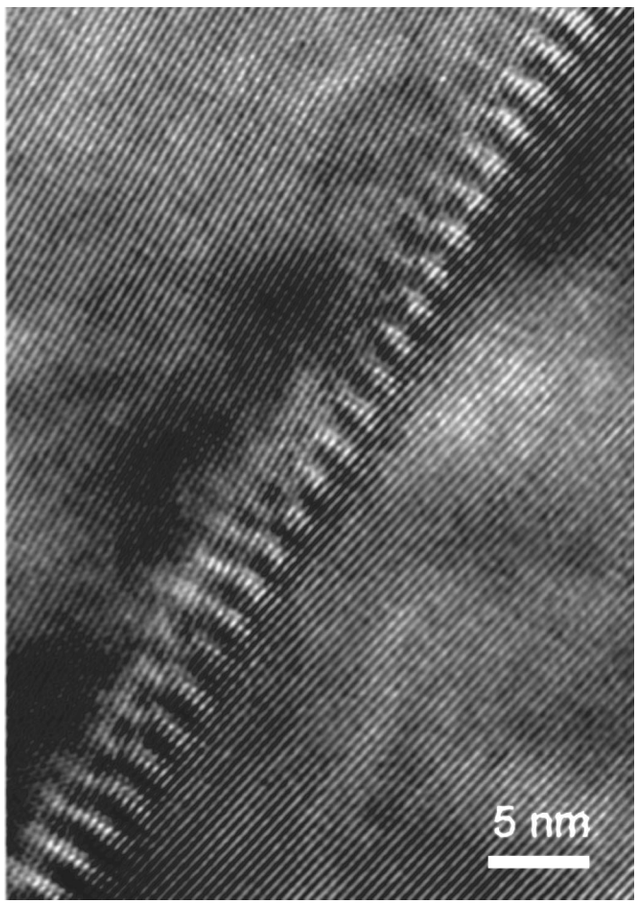

Figure 1. HRTEM of grain boundary in 1.0 mol % Y_2O_3-doped CeO_2. The moiré rings are also visible.

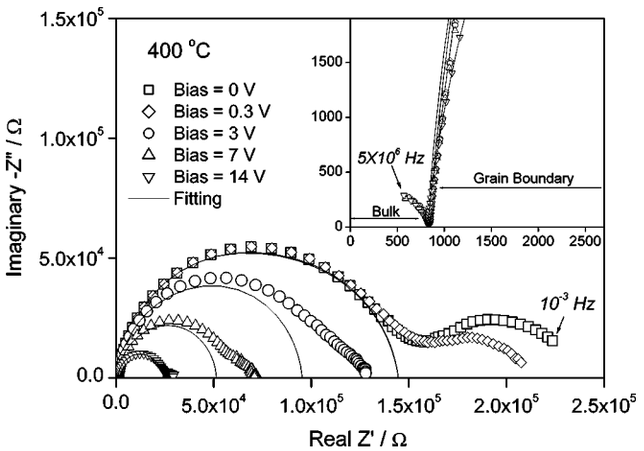

Figure 2. Impedance spectra of 1.0 mol % Y_2O_3-doped CeO_2 at 40°C in air under different dc bias voltages. The bulk arcs are shown in the inset. For clarity, only the fitting results of the grain boundaries are presented.

Results and Discussion

High-purity powders were used to prepare the samples, the grain boundaries of the sintered samples are therefore essentially free of any second phase, as demonstrated by the HRTEM shown in Fig. 1: direct grain-to-grain contacts are prevailing at the grain boundaries. The complexity of the siliceous phase is thus avoided, under such a condition the effect of the space charge layers is dominant at the grain boundaries.[5,6]

Three arcs, corresponding to the impedance responses of the bulk, the grain boundaries, and the electrode, respectively, in order of decreasing frequency, were recorded in the complex impedance spectrum (Fig. 2). Up to 14 V dc bias voltages were applied during the impedance measurements. The bulk properties were independent of bias (Fig. 2), indicating that the sample was not electrochemically degraded. On the contrary, the grain boundary properties were significantly changed under high enough bias voltages (Fig. 2). Assuming cubic grains of the same size and homogeneous grain boundaries (brick-layer model), the bias over one (average) grain boundary is $U_{\text{bias}}R_{\text{gb}}/[(R_{\text{b}} + R_{\text{gb}} + R_{\text{ele}})N_{\text{gb}}]$. Here U_{bias} is the applied dc bias voltage, and R_{b}, R_{gb}, and R_{ele} are the resistances of the bulk, the grain boundaries and the electrode, respectively. The number of the grain boundaries, N_{gb}, in the thickness direction can be calculated from $L/d_{\text{g}} - 1$, with L being the sample thickness and d_{g} the average grain size. The current-bias over one grain boundary relation and the current-applied total bias relation are presented in Fig. 3; both are obviously nonlinear. The nonlinearity coefficient α (=d log I/d log η_{gb}) is 2.0 for the current-bias over one grain boundary curve.

Assuming that the dielectric constants of the bulk and the space charge layers are equal, the effective grain boundary thickness, δ_{gb}, can be calculated from $d_{\text{g}}C_{\text{b}}/C_{\text{gb}}$,[5] with C_{b} and C_{gb} being the capacitances of the bulk and the grain boundaries, respectively. The effective grain boundary thickness *vs.* the bias over one grain boundary relation is plotted in Fig. 4. The effective grain boundary thickness is roughly the combined thickness of two space charge layers. As shown in Fig. 4, the effective thickness increased with increasing bias over one grain boundary. Analogous to electronic conductors,[17] the results given in Fig. 3 and 4 demonstrate that the Schottky barriers are formed at the grain boundaries.

A theoretical model for the dc voltage dependence of the grain boundary electrical properties has been developed for electronic conductors,[17] however, the direct application of such a model to ionic conductors has not yet been justified. One obvious difference

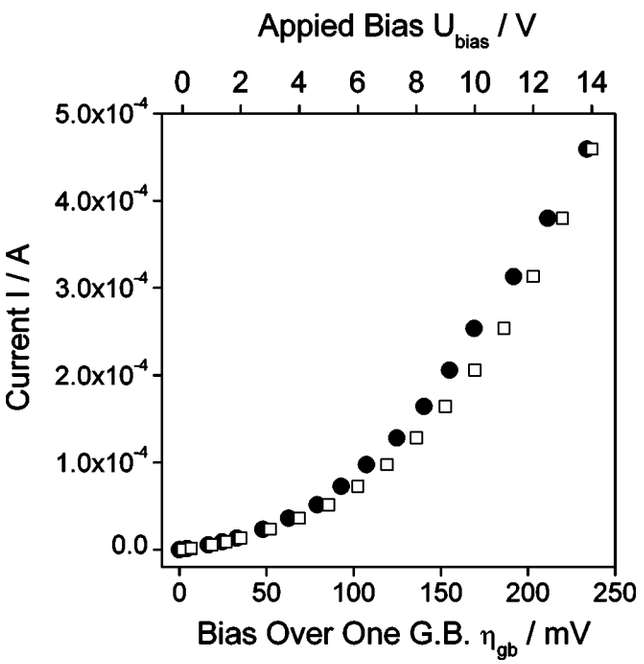

Figure 3. Current I as a function of bias over one grain boundary η_{gb} (filled circles). For comparison the current I-applied bias U_{bias} relation is also plotted (open squares).

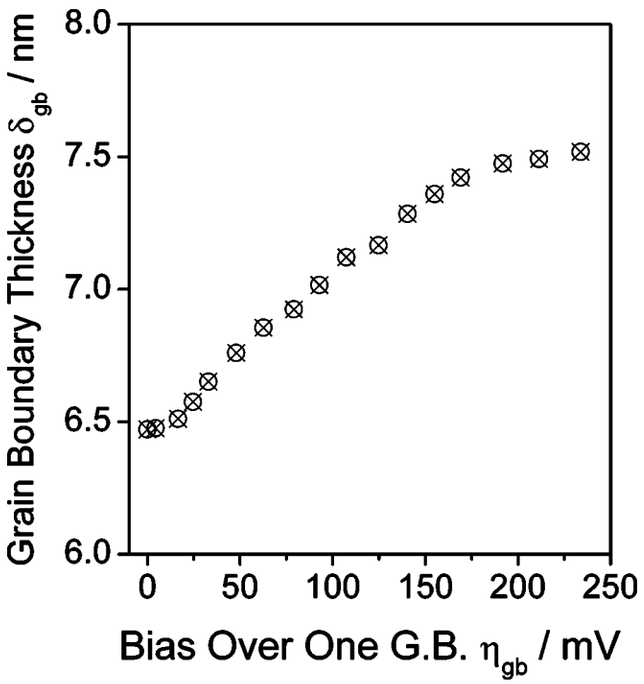

Figure 4. Effective grain boundary thickness δ_{gb} as a function of bias over one grain boundary η_{gb}.

between ionic and electronic conductors is that excessive change of ionic defects, *e.g.*, oxygen vacancies, either in the lattice or at the grain boundaries always results in structure change. Therefore, the density of trap states at the grain boundaries of an ionic conductor is limited. Because of the very small effective grain boundary thickness, a small voltage is already enough to produce high electrical field over one grain boundary; the electrical field ranged mostly from 10^4 to 2×10^5 V cm^{-1} under the experimental conditions, which is high enough to cause the nonlinearity.[17] Similar to electronic conductors, an applied dc bias depresses one of the two space charge layers at a grain boundary, whereas extends the other one. Figure 4 indicates that the overall effect was to increase the combined thickness of the two space charge layers.

Conclusion

The nonlinear dc bias dependence of the grain boundary electrical properties proves the space charge concept. Although the investigation was done on Y_2O_3-doped CeO_2 ceramic, the conclusion is of relevance to all acceptor-doped ZrO_2 and CeO_2.

Institut für Festkörperforschung assisted in meeting the publication costs of this article.

References

1. R. Gerhardt and A. S. Nowick, *J. Am. Ceram. Soc.*, **69**, 641 (1986).
2. M. Gödickemeier, B. Michel, A. Orliukas, P. Bohac, K. Sasaki, L. Gauckler, H. Heinrich, P. Schwander, G. Kostorz, H. Hofmann, and O. Frei, *J. Mater. Res.*, **9**, 1228 (1994).
3. G. M. Christie and F. P. F. Van Berkel, *Solid State Ionics*, **83**, 17 (1996).
4. M. Aoki, Y.-M. Chiang, I. Kosacki, J. R. Lee, H. L. Tuller, and Y.-P. Liu, *J. Am. Ceram. Soc.*, **79**, 1169 (1996).
5. X. Guo and J. Maier, *J. Electrochem. Soc.*, **148**, E121 (2001).
6. X. Guo, W. Sigle, and J. Maier, *J. Am. Ceram. Soc.*, **86**, 77 (2003).
7. J. Maier, *Ber. Bunsenges. Phys. Chem.*, **90**, 26 (1986).
8. S. L. Hwang and I.-W. Chen, *J. Am. Ceram. Soc.*, **73**, 3269 (1990).
9. D. A. Blom and Y.-M. Chiang, *Mater. Res. Soc. Symp. Proc.*, **458**, 127 (1997).
10. C. A. J. Fisher and H. Matsubara, *Comput. Mater. Sci.*, **14**, 177 (1999).
11. Y. Lei, Y. Ito, N. D. Browning, and T. J. Mazanec, *J. Am. Ceram. Soc.*, **85**, 2359 (2002).
12. A. Tschöpe, *Solid State Ionics*, **139**, 267 (2001).
13. S. Kim and J. Maier, *J. Electrochem. Soc.*, **149**, J73 (2002).
14. J.-C. M'Peko, D. L. Spavieri, Jr., and M. F. de Souza, *Appl. Phys. Lett.*, **81**, 2827 (2002).
15. J.-C. M'Peko and M. F. de Souza, *Appl. Phys. Lett.*, **83**, 737 (2003).
16. J. Tanaka, J.-F. Baumard, and P. Abelard, *J. Am. Ceram. Soc.*, **70**, 637 (1987).
17. G. E. Pike and C. H. Seager, *J. Appl. Phys.*, **50**, 3414 (1979).